

Analytical Methods

Accepted Manuscript



This is an *Accepted Manuscript*, which has been through the Royal Society of Chemistry peer review process and has been accepted for publication.

Accepted Manuscripts are published online shortly after acceptance, before technical editing, formatting and proof reading. Using this free service, authors can make their results available to the community, in citable form, before we publish the edited article. We will replace this *Accepted Manuscript* with the edited and formatted *Advance Article* as soon as it is available.

You can find more information about *Accepted Manuscripts* in the [Information for Authors](#).

Please note that technical editing may introduce minor changes to the text and/or graphics, which may alter content. The journal's standard [Terms & Conditions](#) and the [Ethical guidelines](#) still apply. In no event shall the Royal Society of Chemistry be held responsible for any errors or omissions in this *Accepted Manuscript* or any consequences arising from the use of any information it contains.

1
2
3
4 Use of core-shell nanoring amino-functionalized superparamagnetic
5
6 molecularly imprinted polymer for matrix solid phase dispersion extraction
7
8 and preconcentration of BPA in water samples at ultratrace levels water
9

10
11 Ping-Ping Zhan^a, Wen-Jie Gong^b, Yong-Gang Zhao^{c,d,*}

12
13 (^a School of Marine Sciences, Ningbo University, Ningbo, Zhejiang, 315211, China; ^b Cixi
14
15 Municipal Center for Disease Control and Prevention, Ningbo, Zhejiang, 315300, China; ^c
16
17 Zhejiang Provincial Key Laboratory of Health Risk Appraisal for Trace Toxic Chemicals,
18
19 Ningbo Municipal Center for Disease Control and Prevention, Ningbo, Zhejiang, 315010,
20
21 China; ^d Ningbo Key Laboratory of Poison Research and Control, Ningbo Municipal Center
22
23
24
25
26
27 for Disease Control and Prevention, Ningbo, Zhejiang, 315010, China)

28
29 **Abstract:**

30
31 A new method that utilizes core-shell nanoring amino-functionalized magnetic molecularly
32
33 imprinted polymer (CS-NR-MMIP) as an adsorbent for matrix solid phase dispersion
34
35 extraction (MSPD) has been developed for highly selective and sensitive analysis of ultratrace
36
37 BPA (Bisphenol A) by ultra-fast liquid chromatography-tandem mass spectrometry
38
39 (UFLC-MS/MS). The adsorption and desorption conditions including the pH value, shaking
40
41 time, and sample volume were investigated. The results showed the adsorption property of the
42
43 CS-NR-MMIP was highly pH dependent. Under the optimal experimental conditions, the
44
45 enhancement factor of the CS-NR-MMIP MSPD procedure was 250, the limit of quantitation
46
47 (LOQ) was 1 ng·L⁻¹, the linear range was between 1 ng·L⁻¹ and 200 ng·L⁻¹ with a correlation
48
49 coefficient of 0.9992. The results showed that the developed method was faster, easier and
50
51
52
53
54
55

56
57
58

*Corresponding author. Tel.: 086-574-87274559, E-mail address: zhyg91213@163.com (Y.G. Zhao).
59
60

1
2
3
4 more selective for extracting and enriching ultratrace BPA (nanogram per liter level) from
5
6 water samples than the commercial C18 powder.
7

8
9 **Keywords:** Core-shell nanoring amino-functionalized magnetic molecularly imprinted
10 polymer (CS-NR-MMIP), Matrix solid phase dispersion extraction (MSPD), Bisphenol A
11 (BPA), Ultra-fast liquid chromatography–tandem mass spectrometry (UFLC–MS/MS),
12
13 Water
14
15
16
17
18
19

20 21 1. Introduction

22
23 *In vitro* and *in vivo* bioassay studies have shown that bisphenol A (BPA), which is used to
24 fabricate polycarbonate plastics, has estrogenic potency and chronic toxicity [1,2]. BPA is
25 found in clinical (blood, urine, and saliva), food, and water samples in microgram per liter
26 levels [3,4]. In China, BPA is widely present at high concentrations in the urban riverine
27 waters of Guangzhou (65 ng·L⁻¹) and the Liao River system in Northeast China (755.6 ng·L⁻¹)
28 [5,6]. Thus, the preconcentration and analysis of BPA, especially at ultratrace levels in
29 environmental water, is urgently needed for environmental protection, as well as food and
30 agricultural chemistry. However, the direct preconcentration and analysis of BPA in
31 environmental water, especially in drinking water sources, is limited. Therefore, an
32 enrichment and/or separation procedure is necessary to improve BPA preconcentration
33 efficiency, as well as sensitivity and selectivity of analysis.
34
35
36
37
38
39
40
41
42
43
44
45
46
47
48
49
50

51 MSPD is a simple, fast, and inexpensive common technique used for separating and
52 preconcentrating various organic analytes. In the MSPD procedure, the selection of an
53 appropriate adsorbent is a critical factor for obtaining full recovery and high enrichment. For
54
55
56
57
58
59
60

1
2
3 phenols and BPA, many adsorbents have been developed, such as multifunctional
4 biomagnetic capsules [7], polyethersulfone–organophilic montmorillonite hybrid particles [8],
5 activated carbon [9], modified carbon nanotubes [10], acetylaniline-modified
6 hyper-cross-linked polymeric adsorbents [11] and molecularly imprinted particles [12,13].
7
8 However, only a few of these adsorbents are used for the preconcentration and analysis of
9 BPA in water samples at ultratrace levels. A kind of molecularly imprinted layer-coated silica
10 nanoparticles was developed for the extraction and preconcentration of BPA in cosmetic
11 cream samples [14]. SPE using molecularly imprinted layer-coated silica nanoparticles yields
12 satisfactory analyte recovery. However, the use of adsorbents in MSPD involves difficulties
13 with regard to the quick separation of spent adsorbent and shortening of separation time from
14 the solution. Therefore, exploring more suitable adsorbents that can overcome these
15 difficulties, have strong adsorption ability for MSPD, and can enrich BPA at ultratrace levels
16 has become a great challenge.
17
18
19
20
21
22
23
24
25
26
27
28
29
30
31
32
33
34
35

36 Magnetic separation is a useful tool in several areas of applications, such as carriers,
37 immobilizers and separators of biomolecules and drugs, because of its fast recovery, high
38 efficiency, and low cost [15,16]. In our previous work, a kind of core–shell nanoring
39 amino-functionalized magnetic molecularly imprinted polymer adsorbents, named as
40 CS-NR-MMIP had been prepared by ultrasound-assisted suspension polymerization [17]. The
41 CS-NR-MMIP had been verified to be very promising particles for the removal of BPA in
42 wastewater. The maximum adsorption capacity of CS-NR-MMIP to BPA was found to be
43 750.2 mg·g⁻¹. And so, CS-NR-MMIP is expected to be more selective and much stronger
44 adsorption ability than other adsorbents reported in the literature for the MSPD extraction of
45
46
47
48
49
50
51
52
53
54
55
56
57
58
59
60

1
2
3 BPA at ultratrace levels. However, to the best of our knowledge, few such studies have been
4
5 reported so far.
6
7

8
9 The focus of the present research is development and validation of rapid methods for the
10
11 analysis of BPA present in the water samples at ultratrace levels using MSPD followed by
12
13 UFLC-MS/MS analysis. In MSPD, the solid phase adsorbent is thoroughly mixed with
14
15 sample solutions. Dynamic mixing uses less adsorbent and provides faster extractions
16
17 compared to classical SPE. BPA is concentrated on the adsorbent and can be eluted in
18
19 concentrated solution. In this work, the CS-NR-MMIP used as selective adsorbent in MSPD
20
21 for separation and preconcentration of BPA. Parameters that can affect the adsorption and
22
23 recovery efficiency of BPA, such as pH value, the shaking time, the sample volume *etc*, were
24
25 assessed and optimized from laboratory batch tests. Then, the method was applied to the
26
27 analysis of water samples with satisfactory results, which suggests that this method can be
28
29 complimentary to MSPD for separation and preconcentration of phenols in water samples.
30
31
32
33
34
35
36

37 **2. Experimental**

38 **2.1 Reagents and materials**

39
40
41 BPA (> 99%), hexestrol (HEX, > 99%), 4-(tert-octyl)-phenol (4-tOP, > 99%),
42
43 diethylstilbestrol (DES, > 98%), dienestrol (DE, > 99%), and 4-nonylphenol (4-NP, >
44
45 99%) were purchased from Dr. Ehrenstorfer GmbH (Augsburg, Germany). Structural
46
47 formulas are shown in Fig. S1. Ultrapure water was obtained using a MilliQ gradient
48
49 ultrapure water system.
50
51
52
53
54
55
56
57
58
59
60

1
2
3
4 CS-NR-MMIP used in the experiment was prepared in our laboratory according to the
5
6 reported procedure [17]. The paramagnetic Fe_3O_4 was firstly coated with oleic acid. Methyl
7
8 methacrylate (MMA), divinylbenzen (DVB) and glycidylmethacrylate (GMA) were then
9
10 co-polymerized *via* the ultrasound-assisted suspension polymerization procedure over the
11
12 magnetic core to obtain epoxy-functionalized magnetic polymer. Then self-assembly through
13
14 hydrogen bond interaction was conducted by stirring the template (BPA) and active groups,
15
16 i.e., tetraethylenepentamine (TEPA) in methanol. Finally, BPA@TEPA was grafted onto the
17
18 surface of the polymer *via* ring-opening reaction. Thus, the BPA-imprinted CS-NR-MMIP
19
20 was obtained. The template molecules were ultrasonically cleaned with 10% (v/v) acetic acid
21
22 in methanol and methanol. Control core-shell nanoring amino-functionalized magnetic
23
24 nonimprinted polymer (CS-NR-MNIP) nanoparticles were prepared using the same
25
26 procedures described above but without addition of the template. The preparation procedure
27
28 of CS-NR-MMIP was illustrated in Scheme 1. The adsorption capacities of CS-NR-MMIP
29
30 and CS-NR-MNIP for BPA were found to be 750.2 and 125.0 mg/g, respectively [17].
31
32
33
34
35
36
37
38
39
40
41

42 <Insert Scheme. 1>
43
44
45

46 The CS-NR-MMIP obtained was ringed and exhibited a well-defined core-shell
47
48 configuration. The Fe_3O_4 nanoparticles exhibited a uniform morphology with an average
49
50 particle size of about 20 nm. The inside and outside diameters of the ringed CS-NR-MMIP
51
52 were 70 and 150 nm, respectively, and the coated shell had an average thickness of
53
54
55
56
57
58
59
60

1
2
3 approximately 10 nm. CS-NR-MMIP showed a saturation magnetization value of 7.12
4
5
6 emu·g⁻¹.
7
8

9 10 **2.2 Equipment**

11
12 Ultra-fast liquid chromatography-tandem quadrupole mass spectrometry
13 (UFLC-MS/MS) analyses were performed using a Prominence UFLC XR system equipped
14
15 with a DGU-20A3 degasser, a CTO-20AC column oven, a LC-20AD pump, a SIL-20AC
16
17 autosampler (Shimadzu Corporation, Tokyo, Japan) and an AB SCIEX TRIPLE QUAD™
18
19 5500 mass spectrometer (Applied Biosystems, Foster City, CA, USA). The UFLC-MS/MS
20
21 system was controlled and data were analyzed on a computer equipped with Applied
22
23 Biosystems/MDS Sciex Analyst 1.5.1 (Applied Biosystems, Foster City, CA, USA).
24
25
26
27
28
29

30 **2.3 UFLC-MS/MS analysis**

31
32
33 UFLC analysis was performed on a Shim-pack XR-ODS II (100 mm × 2 mm, 2.2 μm)
34
35 using 0.08% ammonia (v/v) in methanol (A) and 0.08% ammonia (v/v) in water (B) as
36
37 eluents in gradient elution. The linear gradient elution was conducted as follows: 0 min to 2
38
39 min, 40% to 70% (A); 2 min to 5 min, 70% to 85% (A); 5 min to 6 min, 85% (A); 6 min to 8
40
41 min, 85% to 40% (A); and 8 min to 9 min, 40% (A). Chromatographic separation was
42
43 conducted at a constant flow rate of 0.45 mL·min⁻¹, with an injection volume of 5 μL. The
44
45 column was thermostated at 40 °C. Mass spectrometry was performed using an electrospray
46
47 ionization source in negative multiple-reaction monitoring (MRM) mode. The operation
48
49 conditions were as follows: -4500 V ion spray voltage, 40 psi curtain gas (with the
50
51 interface heater on), medium collision gas, 50 and 50 psi nebulizer gas (gas 1) and heater gas
52
53
54
55
56
57
58
59
60

(gas 2), 500 °C turbo spray temperature, 10 V entrance potential, 10 V collision cell exit potential, and 50 ms dwell time. Nitrogen was used in all cases. The mass spectrometric information of BPA are shown as follow, the precursor ion: 227.0 (m/z), product ion: 133.0 (m/z) and 211.0 (m/z), corresponding declustering potential (DP): 150 V, and collision energy (CE): 34 eV and 40 eV, respectively. The dwell time was set to 50 ms in the positive mode. Applied Biosystems/MDS Sciex Analyst software (version 1.5.1) was used for data acquisition and processing. Furthermore, the MRM parameters of the five structural analogs, *i.e.*, HEX, 4-tOP, DES, DE and 4-NP for quantification are shown in Table S1.

2.4 Sample preparation

River water was collected from the Yaojiang River, Yongjiang River, and Fenghua River, in Ningbo, China. The pH value of the water sample was adjusted to 7 ± 2 with $0.1 \text{ mol}\cdot\text{L}^{-1}$ HCl and $0.1 \text{ mol}\cdot\text{L}^{-1}$ NaOH, filtered through a polytetrafluoroethylene membrane ($0.45 \mu\text{m}$), and then stored in pre-cleaned polyethylene bottles prior to use. Tap water samples were also collected from our laboratory and analyzed without pretreatment.

2.5 Evaluation of BPA-imprinted CS-NR-MMIP as MSPD adsorbents

2.5.1 Adsorption procedure

Batch adsorption studies were performed by mixing 20 mg of CS-NR-MMIP with 50 mL of BPA solution with varying concentrations from $2 \text{ ng}\cdot\text{L}^{-1}$ to $100 \text{ ng}\cdot\text{L}^{-1}$ in a 100 mL stopper conical flask. HCl ($0.1 \text{ mol}\cdot\text{L}^{-1}$) and NaOH ($0.1 \text{ mol}\cdot\text{L}^{-1}$) solutions were used for pH adjustment. To investigate the effect of pH, 50 mL of 2, 10, and $100 \text{ ng}\cdot\text{L}^{-1}$ BPA with pH ranging from 2 to 11 were mixed with 20 mg CS-NR-MMIP for 24 h to reach equilibrium. To determine the effect of shaking time, 20 mg CS-NR-MMIP was added into 50 mL of 2, 10,

1
2
3 and 100 ng·L⁻¹ BPA under pH 5 to 9, with contact time ranging from 1 min to 120 min. The
4
5 BPA concentration of the samples was measured at specific time intervals. For
6
7 thermodynamic studies, 20 mg CS-NR-MMIP was added into 50 mL of 2, 10, and 100 ng·L⁻¹
8
9 BPA, with temperature ranging from 283.15 K to 323.15 K. When the maximum volume was
10
11 investigated, different volumes of 100 ng·L⁻¹ BPA (5 mL to 100 mL) at pH 5 to 9 were mixed
12
13 with 20 mg CS-NR-MMIP for 30 min to reach equilibrium.
14
15
16
17

18 2.5.2 Elution procedure

19
20 Under adsorption conditions, 20 mg CS-NR-MMIP was mixed with 50 mL of 2, 10, and
21
22 100 ng·L⁻¹ BPA solution in a 100 mL stopper conical flask. After adsorption, the resulting
23
24 adsorbents (BPA-imprinted CS-NR-MMIP) were isolated under the magnetic field and
25
26 washed with 2 mL of water, and then was finally eluted by 200 μL of 0.5%
27
28 ammonia/methanol (v/v) under ultrasound for 1 min. The supernatant concentrated to dryness
29
30 with a nitrogen stream and was redissolved with 200.0 μL of initial mobile phase and filtered
31
32 using a 0.22 μm membrane prior to its injection into the UFLC-MS/MS system.
33
34
35
36
37

38 2.6 Selective extraction comparison

39
40 To evaluate the effectiveness of CS-NR-MMIP for the selective extraction of BPA,
41
42 comparative studies were conducted among three MSPD procedures using CS-NR-MMIP,
43
44 CS-NR-MNIP, and C18 as adsorbents. The various extraction procedures are presented
45
46 below.
47
48
49

50 2.6.1 Extraction with CS-NR-MMIP

51
52 Equal concentrations (10 ng·L⁻¹) of BPA and its five structural analogs, namely, HEX,
53
54 4-tOP, DES, DE, and 4-NP were prepared by appropriate dilution of stock solutions (1
55
56
57
58
59
60

1
2
3
4 mg·L⁻¹) with double-distilled water. Batch adsorption studies were performed by mixing 20
5
6 mg CS-NR-MMIP with 50 mL of the BPA solution mentioned earlier in a 100 mL stopper
7
8 conical flask. The pH of the BPA solution was adjusted to 7±2 with 0.1 M HCl and 0.1
9
10 mol·L⁻¹ NaOH. The mixture was vigorously shaken for 30 min to facilitate the adsorption of
11
12 BPA onto the adsorbents. After adsorption, the BPA-imprinted CS-NR-MMIP was isolated
13
14 under the magnetic field for 1 min and washed with water. Then, the BPA-imprinted
15
16 CS-NR-MMIP was eluted using 200 µL of 0.5% formic acid (v/v) in methanol prior to the
17
18 determination of BPA in aqueous solution by UFLC–MS/MS.
19
20
21
22

23 24 2.6.2 Extraction with CS-NR-MNIP

25
26 The overall procedure was similar to that of CS-NR-MNIP MSPD. However,
27
28 CS-NR-MMIP was replaced with CS-NR-MNIP.
29
30

31 32 2.6.3 Extraction with C18

33
34 The overall procedure was similar to that of CS-NR-MMIP MSPD. CS-NR-MMIP was
35
36 replaced by C18. After the C18 MSPD procedure, the residues and supernatant were
37
38 separated by centrifugation rather than by magnetic separation under a magnetic field.
39
40
41

42 43 2.7 Method validation

44
45 UFLC–MS/MS coupled with CS-NR-MMIP MSPD was developed to determine BPA
46
47 levels because of the low concentration of BPA and the complicated matrix in real samples.
48
49 The matrix-matched calibration curve was constructed by measuring the elution of BPA
50
51 standards in a blank matrix of water after CS-NR-MMIP MSPD in seven different
52
53 concentrations ranging from 1.0 ng·L⁻¹ to 200 ng·L⁻¹. The limit of detection (LOD) and limit
54
55 of quantitation (LOQ) were defined as three- and ten-fold of the signal-to-noise ratio,
56
57
58
59
60

1
2
3
4 respectively. Both the method accuracy and precision were estimated by BPA spiked at
5
6 concentrations of 2.0, 10.0, and 100.0 ng·L⁻¹ in blank samples. The method accuracies were
7
8 expressed as the recoveries, and the method precisions were expressed as the intra-day and
9
10 inter-day relative standard deviations (RSDs). The intra-day RSDs were obtained by repeating
11
12 the three levels of spiked samples nine times within a day, and the inter-day RSDs were
13
14 obtained by repeating the three levels of spiked samples in triplicate on 6 separate days within
15
16 a 2-week period.
17
18
19
20
21

22 **3. Results and discussion**

23 **3.1 FT-IR analysis**

24
25
26
27
28
29 The infrared spectra of CS-NR-MMIP and CS-NR-MNIP nanoparticles were obtained,
30
31 and the results are shown in Fig. 1. The main functional groups of the predicted structures
32
33 can be observed from corresponding infrared absorption peaks. A broad absorption band at
34
35 3440 cm⁻¹ in the spectra of CS-NR-MMIP and CS-NR-MNIP corresponded to stretching
36
37 vibrations of N–H bonds in the amino groups of TEPA molecules. Typical bands of the
38
39 CS-NR-MMIP nanoparticles were observed at 2994 and 2920 cm⁻¹, whereas CS-NR-MNIP
40
41 nanoparticles showed similar bands at 2990 and 2930 cm⁻¹ due to C–H stretching vibrations.
42
43 Other absorption bands, such as those at 1730 (stretching vibrations of C=O bonds on
44
45 carbonyl groups), 1638 (stretching vibrations of C–N bonds), and 1270 and 1150 (stretching
46
47 vibrations of C–O–C bonds of GMA) cm⁻¹ matched the minor peaks of CS-NR-MNIP
48
49 nanoparticles. Furthermore, an absorption band at 563 cm⁻¹ in the spectra of CS-NR-MMIP
50
51 and CS-NR-MNIP corresponded to the Fe–O bond of Fe₃O₄ particles.
52
53
54
55
56
57
58
59
60

<Insert Fig. 1>

3. 2 Effect of pH

To investigate the effect of pH on recovery, 50 mL of 2, 10, and 100 ng·L⁻¹ BPA with pH values ranging from 2 to 11 were mixed with 20 mg CS-NR-MMIP for 24 h to reach equilibrium. The adsorption experiments were conducted in triplicate, and the results are shown in Fig. 2. The adsorption quantity of BPA gradually increased from 22.3% to 94.6%, 35.5% to 97.1%, and 74.1% to 98.4%, with an increase in pH from 2 to 5 at 2, 10, and 100 ng·L⁻¹ BPA, respectively. Above pH 9, the adsorption quantity of BPA decreased with the increase in pH within the studied pH range. The adsorption quantity of BPA increased with the increase in initial BPA concentration from 2 ng·L⁻¹ to 100 ng·L⁻¹, which resulted from the high maximum adsorption capacity of CS-NR-MMIP for BPA (750.2 mg·g⁻¹).

<Insert Fig. 2>

The primary driving forces for the rebinding process, *i.e.*, hydrogen bonding, were strongly related to the sample pH. The state of BPA ($pK_a = 9.7$) and the amino groups (-NH₂, -NH-) of CS-NR-MMIP was influenced by the pH value of the sample. Under acidic conditions (pH < 5.0), the amino groups were easily protonated and in an ionic state, whereas most of the BPAs were in a molecular state. With the increase in pH from 2 to 5, the concentration of H⁺ rapidly decreased. The ability of -NH₂ to be protonated considerably

weakened, thereby increasing the adsorption quantity of BPA. Under alkaline conditions (pH > 9.0), most of the BPAs were in an ionic state, which reduced their adsorption by CS-NR-MMIP. Hydrogen bonding was suppressed in strongly acidic or alkaline solutions because of the ionic state of BPA and amino groups. Therefore, various pH values ranging from 5 to 9 were selected for subsequent experiments.

3.3 Effect of shaking time

Shaking time is an important factor in determining the possibility of applying CS-NR-MMIP for the selective extraction of BPA. To investigate the effect of shaking time on adsorption properties, dynamic adsorption test was performed at different time intervals (1.0-60.0 min). When the shaking time increased from 1.0 min to 20.0 min, the adsorption quantity of BPA increased from 46.86% to 99.22%, 37.80% to 99.92%, and 38.81% to 98.26% for 2, 10, and 100 ng·L⁻¹ BPA, respectively (Fig. S2). The results show that the rate of BPA uptake was initially quite high. Then, a considerably slower adsorption rate was observed, which gradually led to an equilibrium condition.

The adsorption kinetic data obtained from batch experiments were analyzed using a pseudo-second-order rate equation [18] as follows:

$$t/q_t = 1/k_2 q_{e,c}^2 + t/q_{e,c} \quad (3)$$

where q_t is the amount of BPA adsorbed onto the adsorbent at time t (mg/g) and k_2 is the second-order rate constant at equilibrium (g/(mg·min)). By plotting t/q_t against t , the values of k_2 (slope²/intercept), $q_{e,c}$ (1/slope), and $k_2 q_{e,c}^2$ (initial adsorption rate (mg/(g·min)), 1/intercept) can be determined from the slope and intercept of the revealed plots.

In this work, the pseudo-second-order rate equation for the adsorption of BPA onto CS-NR-MMIP nanoparticles was $t/q_t = 0.0226t + 0.0481$ ($R^2 = 0.9996$), which indicates that CS-NR-MMIP possessed rapid adsorption kinetics. BPA adsorption reached the equilibrium within 20 min. Compared with previous studies that suggest a duration of more than 3 h, an incubation period of 30 min was considered sufficient for subsequent studies [8,12,19]. The rapid rebinding kinetics of BPA-imprinted CS-NR-MMIP nanoparticles was attributed to the numerous recognition sites on the surface or near the surface of the particles, which provided easy diffusion of target analytes into the imprinting cavities. Given this feature, BPA-imprinted CS-NR-MMIP nanoparticles are suitable MSPD adsorbents.

3.4 Adsorption thermodynamic studies

To evaluate the thermodynamic parameters for the adsorption of BPA onto CS-NR-MMIP nanoparticles, adsorption studies were conducted from 283.15 K to 323.15 K. When the temperature increased from 283.15 K to 323.15 K, the adsorption quantity of BPA increased from 96.36% to 99.68%, 97.82% to 99.86%, and 98.88% to 99.89% for 2, 10, and 100 ng·L⁻¹ BPA, respectively. The adsorption thermodynamic data obtained from batch experiments were analyzed using Eq. (4) [20],

$$\ln K_D = -\frac{\Delta H^\theta}{RT} + \frac{\Delta S^\theta}{R} \quad (4)$$

where ΔH^θ and ΔS^θ are the values of standard enthalpy change and standard entropy change, respectively. K_D is the distribution coefficient defined by Eq. (5)

$$K_D = \frac{\text{Amount of BPA adsorbed on SCS-Mag-MIP}}{\text{Amount of BPA in solution equilibrium}} \times \frac{V}{m} \quad (5)$$

In this study, the adsorption thermodynamic equation for BPA adsorbed onto

1
2
3 CS-NR-MMIP nanoparticles was $\ln K_D = -1793.7/T + 6.0865$ ($R^2 = 0.9879$). The adsorption
4
5
6 quantity of BPA increased with increased temperature, which indicates that the adsorption of
7
8
9 BPA onto CS-NR-MMIP nanoparticles was endothermic and entropy-favorable in nature.
10
11 Given that BPA can be measured at 303.15 K, this temperature was selected as the optimum
12
13
14 temperature for further studies.

15 16 **3.5 Elution conditions**

17
18 In order to obtain satisfactory recoveries of BPA, a series of eluting agents including 50%
19
20 methanol/water (v/v), 60% methanol/water (v/v), 70% methanol/water (v/v), 80%
21
22 methanol/water (v/v), 90% methanol/water (v/v), methanol, 0.5% ammonia/methanol (v/v)
23
24 and 0.5% acetic acid/methanol (v/v) were evaluated. The results showed that the best
25
26 recoveries (76.2–86.3%) were obtained when 0.5% ammonia/methanol (v/v) and 0.5% acetic
27
28 acid/methanol (v/v) were used as the elution solvent. Furthermore, because 0.08% ammonia
29
30 (v/v) in methanol (A) and 0.08% ammonia (v/v) in water (B) are used as eluents in gradient
31
32 elution, we chose 0.5% ammonia/methanol (v/v) as the elution solvent.

33
34
35
36
37
38 The eluting solvent volume of 100 μL , 200 μL , 300 μL , 400 μL , 500 μL and 600 μL
39
40 was also investigated. The results showed that 200 μL of 0.5% ammonia/methanol (v/v) was
41
42 enough for the elution of BPA from the adsorbents, and the recoveries are in the range of
43
44 79.0-90.2% at the three spiking levels (Fig. S3). In order to improve the recoveries, the
45
46 CS-NR-MMIP capturing BPA was subjected to ultrasound during elution process. The
47
48 ultrasonic time length (0.5-5.0 min) had also been studied and satisfactory recoveries
49
50 (89.2-102.6%) were obtained when 1 min was applied. Therefore, the eluting procedure was
51
52
53
54
55
56
57
58
59
60

1
2
3 carried out with 200 μL of 0.5% ammonia/methanol (v/v) under ultrasound for 1 min after
4
5 optimization.
6
7

8 9 **3.6 Maximum of sample volume and enrichment factor**

10
11 To obtain reliable and reproducible analytical results and a high concentration factor,
12
13 obtaining satisfactory recoveries of the analyte studied from a large volume of sample
14
15 solutions is important. The maximum volume was studied using CS-NR-MMIP MSPD
16
17 procedure with BPA solutions ($100 \text{ ng}\cdot\text{L}^{-1}$) ranging from 5 mL to 100 mL. Following the
18
19 experimental procedure, the recoveries of the analyte at different volumes were obtained, and
20
21 the results indicate that the maximum volume was as high as 50 mL with recovery $> 99.8\%$.
22
23 Furthermore, the similar results were also obtained in medium level of 10.0 ng/g and low
24
25 level of 2.0 ng/g , respectively (Fig. S4). Therefore, 50 mL of the sample solution was adopted
26
27 for the preconcentration of analytes from sample solutions. A high enrichment factor of 250
28
29 was obtained because the final elute solution was $200 \mu\text{L}$ in these experiments.
30
31
32
33
34
35
36

37 38 **3.7 Effect of adsorbent mass and reusability of CS-NR-MMIP**

39
40 In the design of CS-NR-MMIP MSPD procedure, a suitable mass of CS-NR-MMIP that
41
42 had no effect on recovery should be primarily considered. Accordingly, the effects of various
43
44 adsorbent mass on recoveries were studied with tap water sample spiked with 2, 10, and 100
45
46 $\text{ng}\cdot\text{L}^{-1}$ BPA. The spiked samples were preconcentrated using CS-NR-MMIP with different
47
48 masses. The results are shown in Fig. 3. The mass of CS-NR-MMIP adsorbents affected BPA
49
50 recoveries, and a clear trend in the recovery was observed when the adsorbent mass increased
51
52 from 5 mg to 30 mg.
53
54
55
56
57
58
59
60

<Insert Fig. 3>

With the increase in the mass of CS-NR-MMIP adsorbents from 5 mg to 30 mg, the recoveries of BPA increased gradually from 85.0% to 107.6% for the three spiked levels. Thus, the lowest mass of CS-NR-MMIP adsorbents (20 mg) ensured a satisfactory recovery (100.9% to 102.8%) for all concentrations of BPA in this study.

To determine the longevity of the adsorbent, CS-NR-MMIP was subjected to several adsorption and elution experiments. The capacity of the adsorbent was practically constant (variation of 0.8% to 6.2%) after repeated use of more than 50 times. Thus, multiple use of the adsorbent is feasible.

3.8 Selective extraction comparison

The selective extraction of BPA from solutions of BPA and its five structural analogs (HEX, 4-tOP, DES, DE, and 4-NP) was studied. Fig. 4 shows that only BPA was selectively retained on CS-NR-MMIP with almost 100% recovery. C18 showed no retaining selectivity for BPA, as shown by the recoveries for BPA and its structural analogs in the range of 72.6% to 100.2%. BPA and its structural analogs were all poorly retained on CS-NR-MNIP with recoveries of less than 60%. Therefore, BPA-imprinted CS-NR-MMIP adsorbent exhibited high selectivity and molecular recognition function. Although the concentration of each analog was five times that of BPA, the average recovery of BPA was approximately 100%. This result demonstrates that the BPA-imprinted CS-NR-MMIP adsorbent possessed an anti-interference ability. Moreover, the nonspecific binding of HEX to CS-NR-MNIP was very strong, and its recoveries were highest among HEX, 4-tOP, DES, DE, and 4-NP in all

1
2
3
4 situations. Given the presence of two –OH groups in the HEX structure compared with that
5
6 in 4-tOP and 4-NP, HEX easily formed hydrogen bonds with the amino group in
7
8 CS-NR-MNIP. Compared with DES and DE, no –C=C– and –C=C–C=C– groups were
9
10 present in the HEX structure, and HEX was easily adsorbed by CS-NR-MNIP without
11
12 stereospecific blockade. Therefore, HEX presented high recoveries of $42.8\% \pm 2.6\%$ and
13
14 $48.9\% \pm 3.9\%$ with CS-NR-MNIP. HEX did not affect the recovery of BPA by
15
16 CS-NR-MMIP adsorbent despite its strong nonspecific binding. The BPA recoveries
17
18 corresponding to the mixed solutions were $102.2\% \pm 2.7\%$ (1:1) and $99.8\% \pm 1.8\%$ (1:5),
19
20 respectively. The experimental results show that the BPA recoveries in samples containing
21
22 incremental concentrations of HEX were almost 100%.
23
24
25
26
27
28
29
30

31 <Insert Fig. 4>

32 <Insert Table 1>

33
34
35
36
37
38
39 Furthermore, specific selectivity of the CS-NR-MMIP was also carried out with BPA and
40
41 its analogs [21]. Adsorbent (20.0 mg) was dispersed in 50 mL of $0.5 \text{ g}\cdot\text{L}^{-1}$ of BPA and the
42
43 five analogs. Distribution coefficient (K_D), selectivity coefficient (k) and relative selectivity
44
45 coefficient (k') were obtained and the results were listed in Table 1. $K_D = (C_0 - C_e)V/mC_e$,
46
47 where C_0 and C_e ($\text{g}\cdot\text{L}^{-1}$) represent the initial and equilibrium BPA and its analogs
48
49 concentration in the solution. The selectivity coefficient of the adsorbent suggested the
50
51 otherness of two substances adsorbed by one adsorbent, $k = K_D(\text{BPA})/K_D(\text{HEX})$; the relative
52
53 selectivity coefficient suggested the otherness of two adsorbents, $k' = k \text{ MIP}/k \text{ NIP}$. BPA and
54
55
56
57
58
59
60

1
2
3
4 its analogs had similar K_D on the CS-NR-MNIP, but the CS-NR-MMIP showed BPA
5
6 adsorption capacity about five times greater than similar compounds. As shown in Table 1,
7
8 the k value of the CS-NR-MMIP (3.66 for HEX, 7.16 for 4-tOP, 5.30 for DES, 6.42 for DE
9
10 and 7.41 for 4-NP) was larger than that of the CS-NR-MNIP (0.709 for HEX, 1.83 for 4-tOP,
11
12 1.73 for DES, 1.36 for DE and 3.04 for 4-NP), which showed that the CS-NR-MMIP had
13
14 high selectivity for BPA over the analogs. The relative selectivity coefficient was 5.2 for
15
16 HEX, 3.9 for 4-tOP, 3.1 for DES, 4.7 for DE and 2.4 for 4-NP, which shows the high
17
18 selectivity of the CS-NR-MMIP than the CS-NR-MNIP.
19
20
21
22
23
24

25 **3.9 Method validation and application to real samples**

26
27 Under the optimized conditions for UFLC–MS-MS coupled with CS-NR-MMIP MSPD,
28
29 the correlation coefficient of the calibration curve was excellent ($r = 0.9992$) in the
30
31 concentration range of $1 \text{ ng}\cdot\text{L}^{-1}$ to $200 \text{ ng}\cdot\text{L}^{-1}$. LOD and LOQ were 0.3 and $1 \text{ ng}\cdot\text{L}^{-1}$,
32
33 respectively. The accuracy of the method was estimated by determining river water and tap
34
35 water samples spiked with BPA at three different concentration levels. The method robustness
36
37 has been indicated by two analysts who used two analytical columns and two LC-MS-MS
38
39 plate-forms during the analysis of real samples.
40
41
42
43
44
45
46
47
48
49
50
51
52
53
54

55 <Insert Table 2>

56 <Insert Table 3>

57
58 The proposed MSPD UFLC–MS-MS method was used to determine ultratrace BPA in
59
60 river water and tap water samples. The results are listed in Table 2. The average recoveries by

1
2
3
4 the MSPD method for river water and tap water were 90.0% to 107% with relative standard
5
6 deviation < 10%. These results indicate the suitability of CS-NR-MMIP for selective MSPD
7
8 and determination of ultratrace BPA in environmental water samples. Furthermore, a
9
10 comparison study among different methods for the determination of BPA applied in water
11
12 samples was also outperformed, and the results are shown in Table 3. The CS-NR-MMIP
13
14 need not to be packed into the SPE cartridge but dispersed in the sample instead. Extraction
15
16 and enrichment, the two most time-consuming procedures in sample pretreatment, could be
17
18 fulfilled simultaneously by simply blending and stirring the sample, and the use of
19
20 CS-NR-MMIP. As is shown in the table, the proposed method gives a simpler and faster way
21
22 for the extraction of BPA in water samples and provides a relatively lower LOD, higher
23
24 recoveries of BPA and better precisions.
25
26
27
28
29
30
31
32

33 34 **4. Conclusion**

35
36 For the first time, magnetic isolate was used in the MSPD with magnetic polymeric
37
38 particles(CS-NR-MMIP) for separation/preconcentration of BPA at ultratrace in water
39
40 samples, which can separate the adsorbed adsorbent quickly and shorten the separation time
41
42 from the solution. This simple, fast and cost effective procedure is based on the adsorption of
43
44 BPA onto CS-NR-MMIP by hydrogen bond interaction. The enrichment method allowed
45
46 BPA determination in different aqueous samples with good accuracy and reproducibility. The
47
48 proposed MSPD UFLC–MS/MS method was highly sensitive and selective for BPA in
49
50 environmental water samples, with LOD at nanogram per liter level.
51
52
53
54
55
56

57 58 **Acknowledgements**

59
60

We would like to thank the National Natural Science Foundation of China (No. 21377114), the Agriculture and Social Development Funds of Ningbo, China (No. 2011C50058), the Zhejiang Provincial Analytical Foundation of China (No. 2012C37002, No. 2014C37037), the Medical Science and Technology Funds of Ningbo (No. 2011A07), the Zhejiang Provincial Natural Science Foundation (No. LY12H26003) and Zhejiang Provincial Program for the Cultivation of High-level Innovative Health Talents.

References

- [1] A. Can, O. Semiz, O. Cinar, *Mol. Hum. Reprod.* 11 (2005) 389.
- [2] T. Funabashi, T.J. Nakamura, F. Kimura, *J. Neuroendocrinol.* 16 (2004) 99.
- [3] W. Dekant, W. Voelkel, *Toxicol. Appl. Pharm.* 228 (2008) 114.
- [4] W. Volkel, M. Kiranoglu, H. Fromme, *Toxicol. Lett.* 179 (2008) 155.
- [5] L. Wang, G.G. Ying, J.L. Zhao, S. Liu, B. Yang, L.J. Zhou, R. Tao, H.C. Su, *Environ. Pollut.* 159 (2011) 148.
- [6] X. Peng, Y. Yu, C. Tang, J. Tan, Q. Huang, Z. Wang, *Sci. Total Environ.* 397 (2008) 158.
- [7] C.R. Ispas, M.T. Ravalli, A. Steere, S. Andreescu, *Water Res.* 44 (2010) 1961.
- [8] F. Cao, P. Bai, H. Li, Y. Ma, X. Deng, C. Zhao, *J. Hazard. Mater.* 162 (2009) 791.
- [9] I. Bautista-Toledo, M.A. Ferro-García, J. Rivera-Utrilla, C. Moreno-Castilla, F.J. Vegas-Fernández, *Environ. Sci. Technol.* 39 (2005) 6246.
- [10] C.Y. Kuo, *Desalination* 249 (2009) 976.
- [11] G. Xiao, L. Fu, A. Li, *Chem. Eng. J.* 191 (2012) 171.
- [12] Y. Ren, W. Ma, J. Ma, Q. Wen, J. Wang, F. Zhao, *J. Colloid Interf. Sci.* 367 (2012) 355.

- 1
2
3
4 [13] M.B. Gholivand, M. Shamsipur, S. Dehdashtian, H.R. Rajabi, *Mater. Sci. Eng. C* 36
5
6 (2014) 102-107.
7
8
9 [14] R. Zhu, W. Zhao, M. Zhai, F. Wei, Z. Cai, N. Sheng, Q. Hu, *Anal. Chim. Acta* 658
10
11 (2010) 209.
12
13 [15] F.C. Meldrum, B.R. Heywood, S. Mann, *Science* 257 (1992) 522.
14
15 [16] M.V. Kiselev, A.K. Gladilin, N.S. Melik-Nubarov, P.G. Sveshnikov, P. Miethe, A.V.
16
17 Levashov, *Anal. Biochem.* 269 (1999) 393.
18
19 [17] Y.G. Zhao, X.H. Chen, S.D. Pan, H. Zhu, H.Y. Shen, M.C. Jin, *J. Mater. Chem. A* 1
20
21 (2013) 11648.
22
23 [18] Y.S. Ho, G. Mckay, *Process Biochem.* 34 (1999) 451.
24
25 [19] B. Yu, X. Zhang, J. He, K. Yang, C. Zhao, *J. Appl. Polym. Sci.* 108 (2008) 3859.
26
27 [20] S.P. Ramnani, S. Sabharwal, *React. Funct. Polym.* 66 (2006) 902.
28
29 [21] Y.K. Lv, J.Q. Zhang, Y.D. He, J. Zhang, H.W. Sun, *New J. Chem.* 38 (2014) 802.
30
31 [22] R. Loos, G. Hanke, G. Umlauf, S.J. Eisenreich, *Chemosphere* 66 (2007) 690.
32
33 [23] A. Laganà, A. Bacaloni, I.D. Leva, A. Faberi, G. Fago, A. Marino, *Anal. Chim. Acta*
34
35 501 (2004) 79.
36
37 [24] T. Vega-Morales, Z. Sosa-Ferrera, J.J. Santana-Rodríguez, *J. Hazard. Mater.* 183 (2010)
38
39 701.
40
41 [25] H. Sambe, K. Hoshina, K. Hosoya, J. Haginaka, *J. Chromatogr. A* 1134 (2006) 16.
42
43
44
45
46
47
48
49
50
51
52
53
54
55
56
57
58
59
60

Tables Captions

Table 1 Distribution coefficient (K_D), selectivity (k) and relative selectivity (k') obtained by competitive adsorption of BPA and its five structural analogs on CS-NR-MMIP and CS-NR-MNIP

Table 2 Determination of ultratrace levels of BPA in river water and tap water samples using CS-NR-MMIP MSPD UFLC–MS-MS

Table 3 Comparison of the analytical features of current LC-MS-based methodologies for the determination of BPA in water samples

Table 1 Distribution coefficient (K_D), selectivity (k) and relative selectivity (k') obtained by competitive adsorption of BPA and its five structural analogs on CS-NR-MMIP and CS-NR-MNIP

Analyte	$C_0(\text{g}\cdot\text{L}^{-1})$	$C_e(\text{g}\cdot\text{L}^{-1})$		K_D		k		k'
		CS-NR-MMIP	CS-NR-MNIP	CS-NR-MMIP	CS-NR-MNIP	CS-NR-MMIP	CS-NR-MNIP	
BPA	0.500	0.351	0.468	1.06	0.171	—	—	—
HEX	0.500	0.448	0.456	0.29	0.241	3.66	0.709	5.2
4-tOP	0.500	0.472	0.482	0.148	0.0933	7.16	1.83	3.9
DES	0.500	0.463	0.481	0.200	0.0988	5.30	1.73	3.1
DE	0.500	0.469	0.476	0.165	0.126	6.42	1.36	4.7
4-NP	0.500	0.473	0.489	0.143	0.0561	7.41	3.04	2.4

Table 2 Determination of ultratrace levels of BPA in river water and tap water samples using CS-NR-MMIP MSPD UFLC–MS-MS

CS-NR-MMIP MSPD UFLC–MS-MS				
Sample	Added (ng·L ⁻¹)	Found (ng·L ⁻¹)	Accuracy ^a (%)	Precision (RSD, %)
	0	20.3	-	-
Yaojiang	1	21.2	90.0	2.9 ^b , 4.2 ^c
water	10	31.0	107	5.9, 5.3
	100	123	103	3.6, 6.3
	0	16.3	-	-
Fenghuajiang	1	17.3	100	2.6, 3.9
water	10	26.2	99.0	5.3, 6.1
	100	120	104	2.8, 5.5
	0	2.26	-	-
Tap water	1	3.28	102	5.6, 6.2
	10	13.0	107	4.6, 7.6
	100	100	97.7	8.2, 9.2

^a The mean value was determined in one day ($n = 9$ replicates).

^b Intra-day, $n = 9$ replicates.

^c Inter-day, $n = 3$ replicates \times 6 days within a 2-week period.

Table 3 Comparison of the analytical features of current LC-MS-based methodologies for the determination of BPA in water samples

Sample	Sample preparation (main steps)	Detection	Recovery (%)	R.S.D.(%)	Method LOD (ng·L ⁻¹)	reference
Waste water treatment plant effluents and surface waters	HLB SPE	LC-MS/MS	—	—	2.0	[22]
Sewage treatment plants and natural waters	HLB SPE	LC-MS/MS	99.0-102%	2.0-4.0	0.2-3.0	[23]
Sewage samples	C ₁₈ SPE	LC-MS/MS	73.0-93.0 %	7.0-13	1.9-9.8	[24]
River	RAM-MIP SPE	LC-MS	86.4-103%	0.83-3.3	5.0	[25]
River	CS-NR-MMIP MSPD	LC-MS/MS	96.0-120%	2.6-9.2	0.30	This work

Scheme and Figures Captions

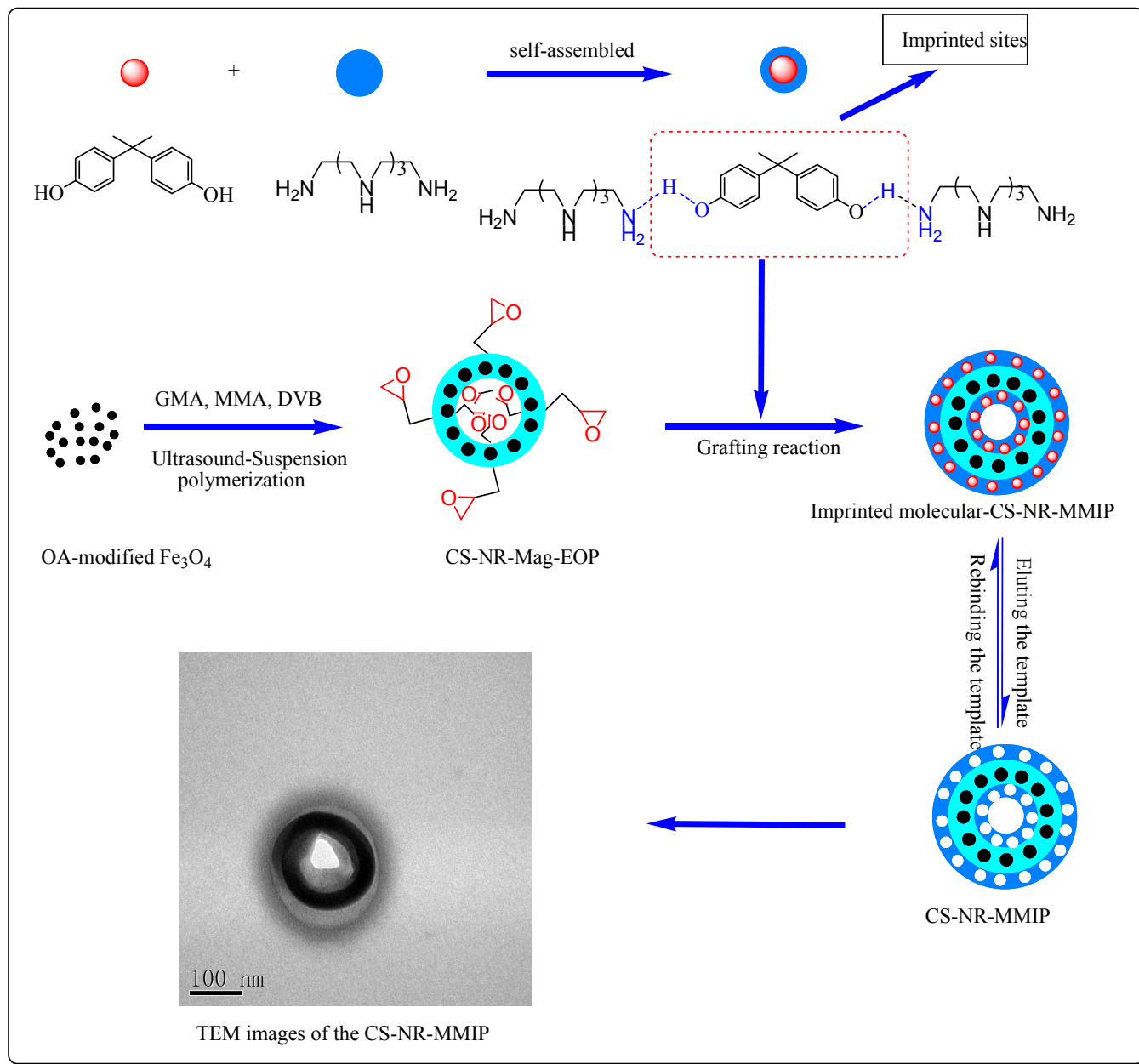
Scheme 1 Schematic procedures for the self-assembly of surface bisphenol A-imprinted CS-NR-MMIP nanoparticles.

Fig. 1 FTIR spectra of CS-NR-MMIP and CS-NR-MNIP nanoparticles

Fig. 2 Effect of pH on BPA recovery using CS-NR-MMIP.

Fig. 3 Effect of the amount of CS-NR-MMIP on BPA recovery.

Fig. 4 Recoveries of BPA and its analogs after C18 MSPD, CS-NR-MMIP MSPD, and CS-NR-MNIP MSPD (the concentration of each analyte was $10 \text{ ng}\cdot\text{L}^{-1}$)



Scheme 1 Schematic procedure for the self-assembly of surface bisphenol

A-imprinted CS-NR-MMIP nanoparticles.

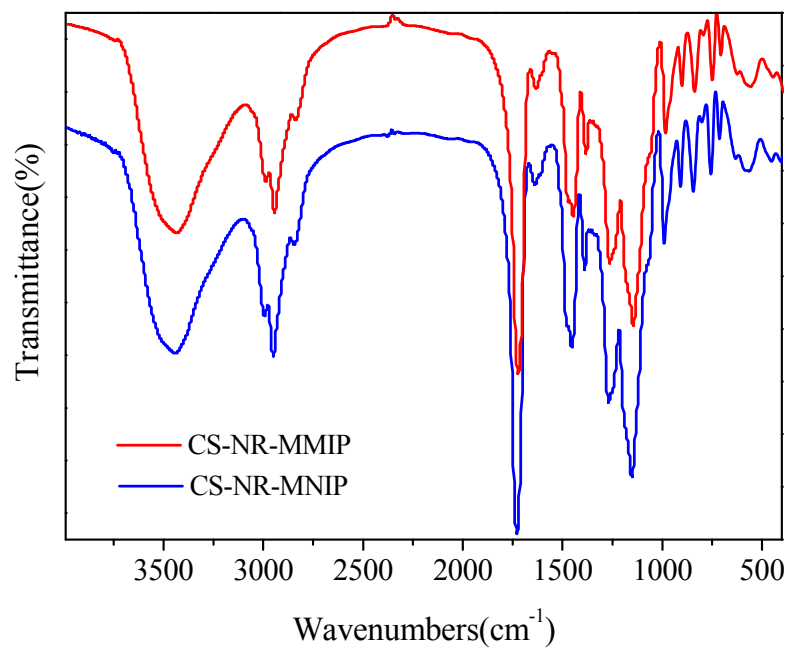


Fig. 1 FTIR spectra of CS-NR-MMIP and CS-NR-MNIP nanoparticles

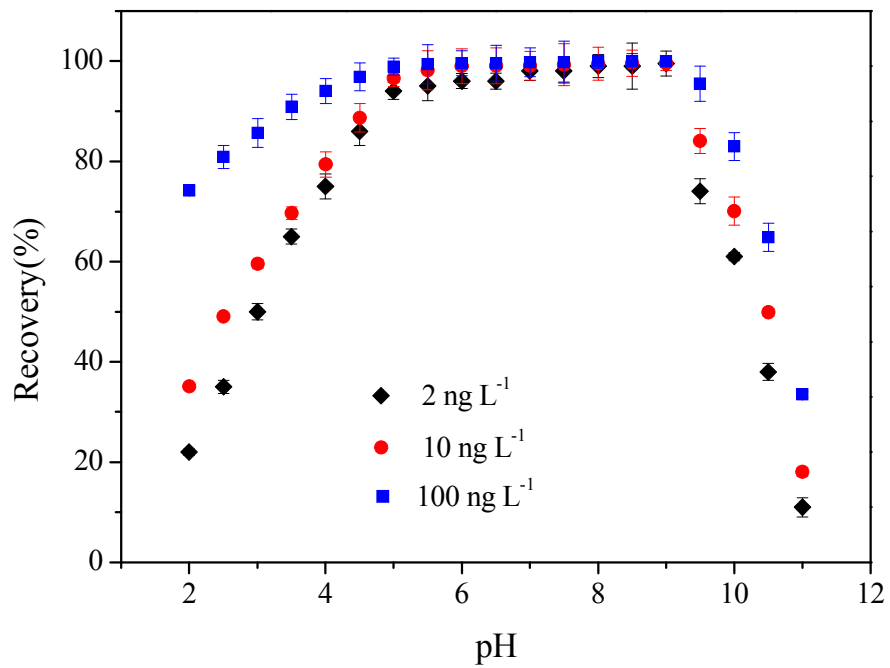


Fig. 2 Effect of pH on BPA recovery using CS-NR-MMIP.

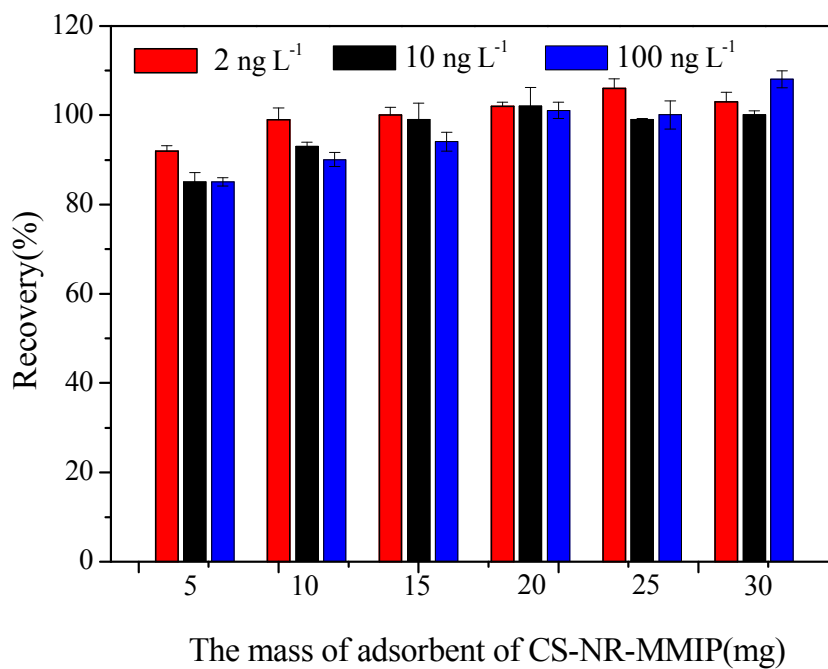


Fig. 3 Effect of the amount of CS-NR-MMIP on BPA recovery.

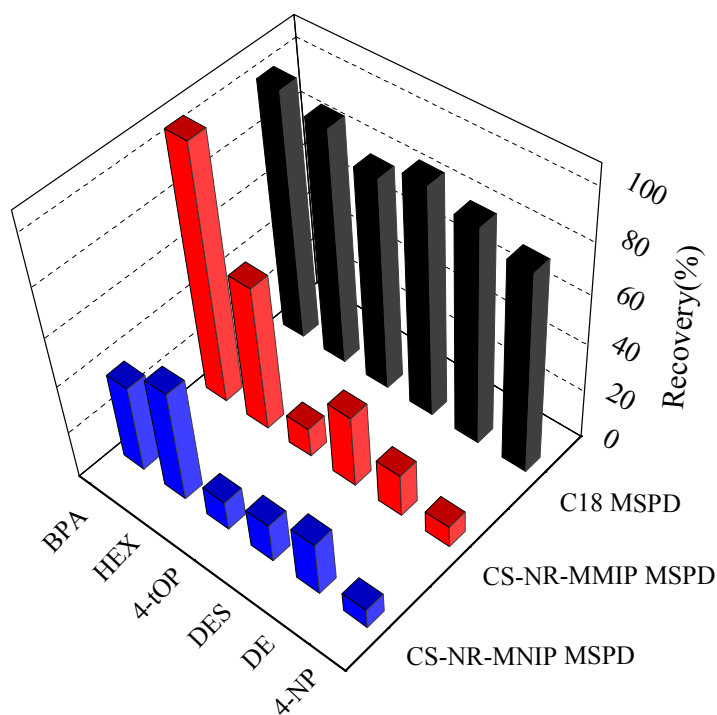


Fig. 4 Recoveries of BPA and its analogs after C18 MSPD, CS-NR-MMIP MSPD, and CS-NR-MNIP MSPD (the concentration of each analyte was $10 \text{ ng} \cdot \text{L}^{-1}$)

Supporting Information

Table S1. Q1/Q3 ion pairs, declustering potential (DP), and collision energy (CE) from multiple-reaction monitoring and retention time for five structural analogs.

Fig. S1. Structural formulas of BPA and its five structural analogs.

Fig. S2. Effect of the shaking time on BPA recovery.

Fig. S3. Effect of the volume of eluting solvent on BPA recovery.

Fig. S4. Effect of the volume of sample on BPA recovery.

Table S1. Q1/Q3 ion pairs, declustering potential (DP), and collision energy (CE) from multiple-reaction monitoring and retention time for five structural analogs

Compounds	Precursor ion (Q1, m/z)	Fragment ion (Q3, m/z)	DP (V)	CE (eV)	Retention Time (min)
DES	267.1	251.1*, 237.1	140, 140	32, 37	3.46
DE	265.2	93.0*, 171.0	130, 130	31, 25	3.59
HEX	269.1	134.1*, 119.0	130, 130	20, 51	3.69
4-tOP	205.0	133.0*, 93.0	120, 120	32, 60	5.54
4-NP	219.0	106.0*, 119.0	100, 100	26, 55	7.09

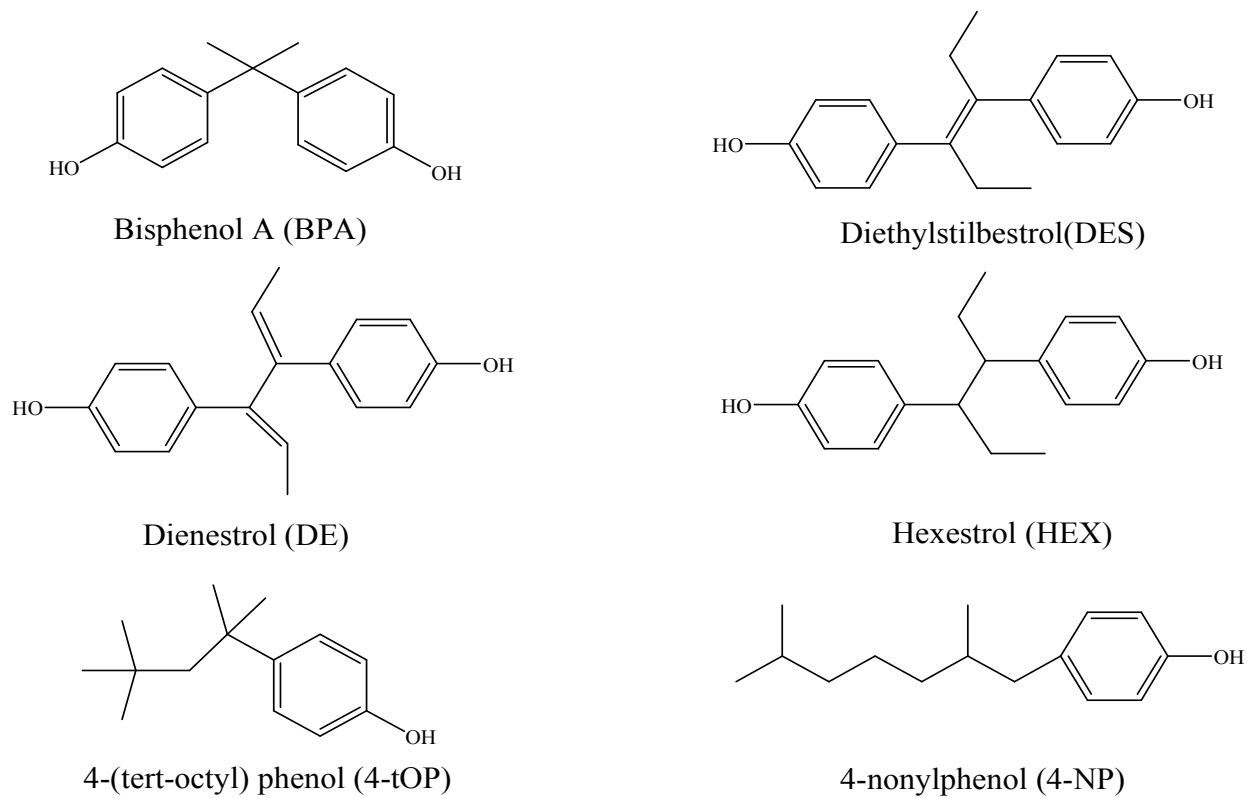


Fig. S1. Structural formulas of BPA and its five structural analogs

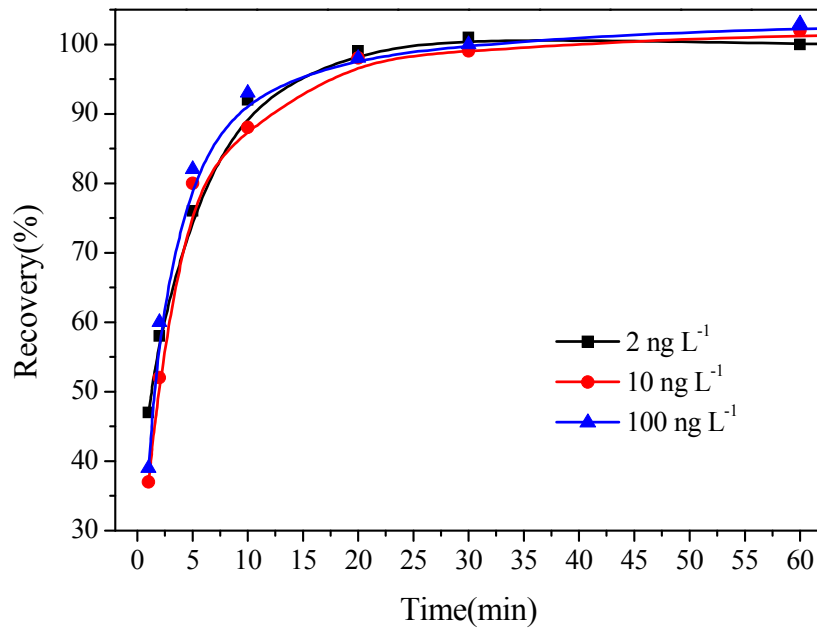


Fig. S2. Effect of the shaking time on BPA recovery.

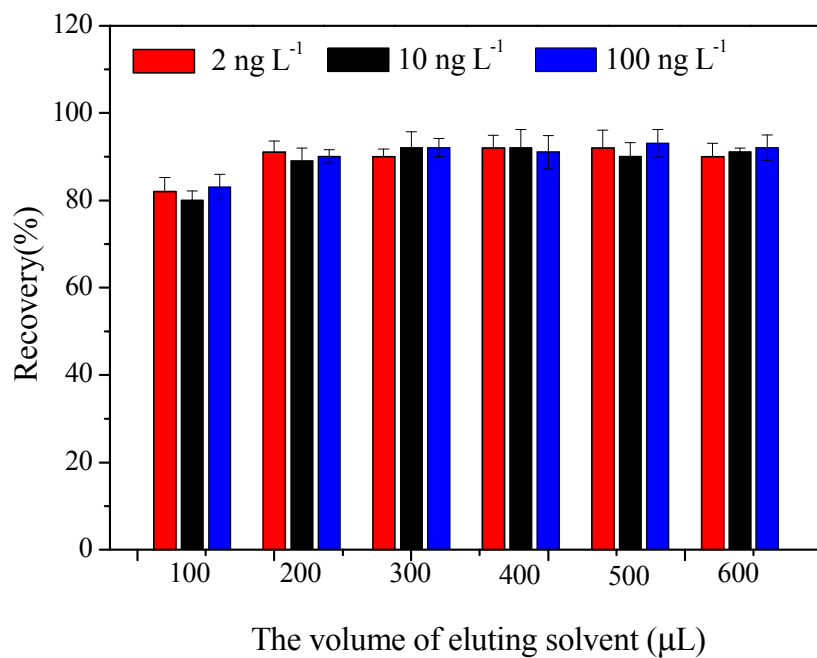


Fig. S3. Effect of the volume of eluting solvent on BPA recovery.

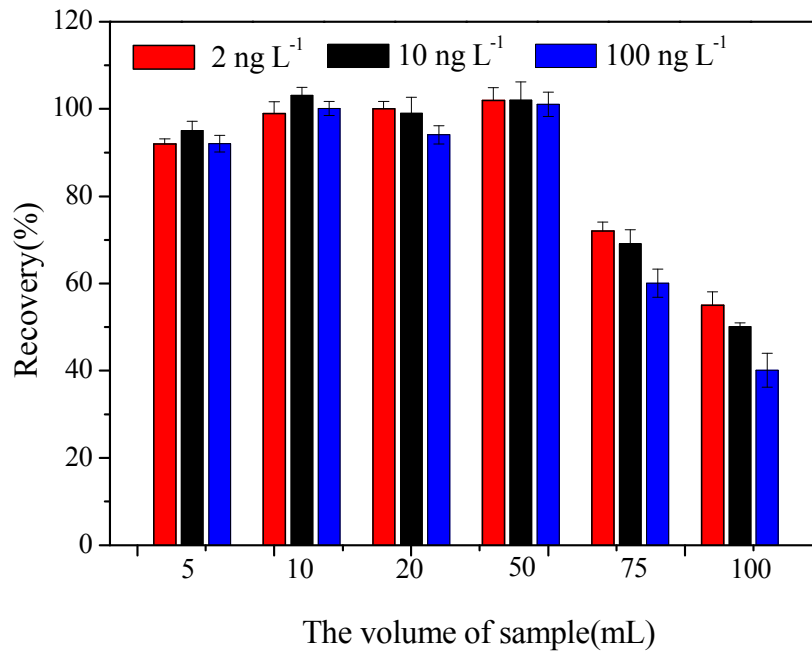


Fig. S4. Effect of the volume of sample on BPA recovery.